Science of the Total Environment 741 (2020) 140467

Contents lists available at ScienceDirect

Science of the Total Environment

journal homepage: www.elsevier.com/locate/scitotenv

Changes in ozone and $PM_{2.5}$ in Europe during the period of 1990–2030: Role of reductions in land and ship emissions

Jianhui Jiang [a,*], Sebnem Aksoyoglu [a,*], Giancarlo Ciarelli [b,c], Urs Baltensperger [a], André S.H. Prévôt [a]

[a] Laboratory of Atmospheric Chemistry, Paul Scherrer Institute, 5232 Villigen PSI, Switzerland
[b] Department of Chemical Engineering, Carnegie Mellon University, Pittsburgh, PA, USA
[c] Now at: Institute for Atmospheric and Earth System Research/Physics, Faculty of Science, University of Helsinki, Finland

HIGHLIGHTS

- Modeled effects of emission reductions in Europe on O_3 and $PM_{2.5}$ during 1990–2030
- Decline in days with maximum daily 8-h average ozone >60 ppb by up to 53%
- Reduction of domain average $PM_{2.5}$ by ~56% between 1990 and 2030
- Decrease in $PM_{2.5}$ mainly due to sulfate before 2020 while due to nitrate after 2020
- Up to 19% decrease in $PM_{2.5}$ over land due to reduced ship emissions by 2030

GRAPHICAL ABSTRACT

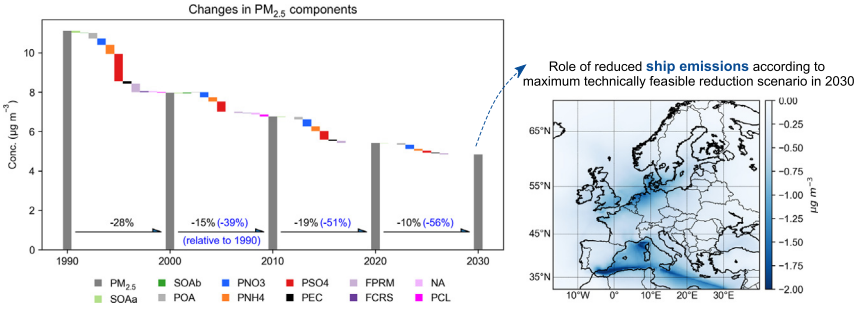

ARTICLE INFO

Article history:
Received 24 March 2020
Received in revised form 21 June 2020
Accepted 22 June 2020
Available online 23 June 2020

Editor: Jianmin Chen

Keywords:
Ozone
$PM_{2.5}$
Ship emissions
CAMx
Europe

ABSTRACT

Air pollution is among the top threats to human health and ecosystems despite the substantial decrease in anthropogenic emissions. Meanwhile, the role of ship emissions on air quality is becoming increasingly important with the growing maritime transport and less strict regulations. In this study, we modeled the air quality in Europe between 1990 and 2030 with ten-year intervals, using the regional air quality model CAMx version 6.50, to investigate the changes in the past (1990–2010) as well as the effects of different land and ship emission scenarios in the future (2020,2030). The modeled mean ozone levels decreased slightly during the first decade but then started increasing again especially in polluted areas. Results from the future scenarios suggest that by 2030 the peak ozone would decrease, leading to a decrease in the days exceeding the maximum daily 8-h average ozone (MDA8) limit values (60 ppb) by 51% in southern Europe relative to 1990. The model results show a decrease of 56% (6.3 μg m^{-3}) in $PM_{2.5}$ concentrations from 1990 to 2030 under current legislation, mostly due to a large drop in sulfate (representing up to 44% of the total $PM_{2.5}$ decrease during 1990–2000) while nitrate concentrations were predicted to go down with an increasing rate (10% of total $PM_{2.5}$ decrease during 1990–2000 while 36% during 2020–2030). The ship emissions if reduced according to the maximum technically feasible reduction (MTFR) scenario were predicted to contribute up to 19% of the decrease in the $PM_{2.5}$ concentrations over land between 2010 and 2030. Ship emission reductions according to the MTFR scenario would lead to a decrease in the days with MDA8 exceeding EU limits by 24–28% (10–14 days) around the coastal regions. The results obtained in our study show the increasing importance of ship emission reductions, after a relatively large decrease in land emissions was achieved in Europe.

* Corresponding authors.
E-mail addresses: jianhui.jiang@psi.ch (J. Jiang), sebnem.aksoyoglu@psi.ch (S. Aksoyoglu).

https://doi.org/10.1016/j.scitotenv.2020.140467

1. Introduction

Air pollution is considered as the greatest environmental risk to human health by the World Health Organization (WHO, 2019). Despite considerable reductions in emissions of air pollutants under numerous pollution control regulations, air pollution remains to be a critical issue in many areas. Due to the complex links between emissions and air quality, reductions of emissions do not have always a linear effect on concentrations, especially for pollutants such as ozone (O_3) and fine particulate matter with an aerodynamic diameter smaller than 2.5 μm ($PM_{2.5}$). Although anthropogenic emissions of air pollutants have been substantially reduced in Europe since 1990s according to the Gothenburg Protocol (UNECE, 1999), ground-level ozone and particulate matter are still the most problematic pollutants with adverse effects on human health and ecosystems (EEA, 2019a). A significant increase has been observed in the annual mean ozone levels since 1995 (Yan et al., 2018). On the other hand, approximately 77% of the population was still exposed to $PM_{2.5}$ concentrations exceeding the WHO air quality guidelines (AQG) in 2017 (EEA, 2019a). Therefore, understanding the effects of emission reductions on ozone and $PM_{2.5}$ concentrations is crucial for emission control strategies for the future.

Ground level ozone is formed in the atmosphere through various chemical reactions of its precursors nitrogen oxides (NO_x) and volatile organic compounds (VOCs) in the presence of sunlight (Sillman, 1999). The surface ozone mixing ratio is sensitive to the changes in its precursor concentrations, and the effects are non-linear and highly uncertain (Oikonomakis et al., 2018a). The response of ozone to the reduced NO_x and VOC emissions for different areas and time periods have been widely investigated by model and measurement based studies. It is generally found that summertime ozone peaks have decreased but wintertime ozone especially in the urban areas increased due to the reduced NO titration (Aksoyoglu et al., 2014; Barna et al., 2001; Jimenez and Baldasano, 2004; Li et al., 2013; Pollack et al., 2013; Wei et al., 2019). However, the effects of reduced emissions on ozone mixing ratios largely depend on the levels of NO_x and VOC, as well as their ratio (Monks et al., 2015; Sillman, 1999). Thus, how the changing emissions will influence the future surface ozone remains to be investigated.

The other important pollutant posing high risk to human health, $PM_{2.5,}$ originates from primary particles directly emitted to the atmosphere and secondary formation through reactions of multiple precursor gases, i.e. SO_2, NO_x, NH_3 and VOCs. The largest decrease in the emissions of the EU countries since 1990s was seen for SO_x emissions (decreasing by 91% from 1990 to 2017) followed by anthropogenic VOC (61%) and NO_x (58%) emissions, while the decrease in ammonia emissions (24%) has been relatively small (EEA, 2019b). According to the WHO database, about 90% of the population living in cities are exposed to $PM_{2.5}$ values exceeding the AQG in 2016 (WHO, 2016). In Europe, the first EU Directive on air quality limit values (80/779/EEC) set the limit for PM in terms of total suspended particulate matter (TSP). In 2008 the Air Quality Directive 2008/50/EC specified the limit values for ambient PM_{10} and $PM_{2.5}$ (which was transformed into a legally binding limit in January 2015 for $PM_{2.5}$). The PM_{10} concentrations show on average a decreasing trend over the last couple of decades as a consequence of reductions of primary PM and precursor emissions, however, trend analyses for $PM_{2.5}$ are difficult due to the limited spatial and temporal availability of $PM_{2.5}$ data (Guerreiro et al., 2014). All evidence indicates the necessity to investigate the changes in ozone and $PM_{2.5}$ concentrations with changing emissions at a higher spatial and temporal coverage.

While anthropogenic emissions on land have been decreasing substantially since the 1990s due to regulations in Europe, emissions from one of the least regulated sector, i.e., marine transportation, have continued to increase (EEA, 2013). The role of ship emissions on air quality is therefore becoming more and more important with the growth of international trade (Aksoyoglu et al., 2016; Aulinger et al., 2016; Chen et al., 2019; Karl et al., 2019; Lv et al., 2018; Mamoudou et al., 2018; Mertens et al., 2018; Monteiro et al., 2018; Nakatsubo et al., 2020; Viana et al., 2014). Viana et al. (2014) reviewed the impacts of ship emissions on coastal air quality in Europe, and found that the annual mean contribution of ship emissions to $PM_{2.5}$ varied between 1 and 14%, with a summer maximum of 20% in Genoa, Italy. Especially for the secondary components of $PM_{2.5}$ such as sulfate, the ship emissions could contribute up to 60% in the Mediterranean and 30–35% in the English Channel and the North Sea (Aksoyoglu et al., 2016). The effect of ship emissions on ozone is relatively lower compared to $PM_{2.5}$, but the influence could extend to areas far away from the coast (Monteiro et al., 2018). Meanwhile, Matthias et al. (2016) reported that the contribution of ship emissions to increased ozone levels might be enhanced in the future by more than 20% far from the main shipping areas in Central Europe, Ireland and northern UK. Despite the considerable contribution of ship emissions on air quality, the regulations on ship emissions started much later compared to those for land emissions (Crippa et al., 2016). The most important legislation on ship emissions, International Convention for the Prevention of Pollution from Ships (MARPOL) Annex VI "Regulations for the Prevention of Air Pollution from Ships", entered into force on May 2005. It was revised in 2008 to include the Tier II and III emission standards, which required to reduce the sulfur content of marine fuels from 4.5% to 3.5% (effective from January 2012 for Tier II), and progressively to 0.5% by January 2020 for Tier III (IMO, 2008b). More stringent limits were applied in the Emission Control Areas (ECAs), i.e. the Baltic Sea, the North Sea and the English Channel in Europe, where the sulfur content had to be reduced to 0.1% in 2015. The NO_x emission limits for Tier II apply to all ship diesel engines of over 130 kW constructed in or after 2011 (IMO, 2008a). For ECAs in Europe, the Tier III NO_x requirements will be applied for ships constructed after January 2021, which is expected to reduce the NO_x emissions by ~75% compared to Tier II. While understanding the potential effects of these stricter ship emission regulations on future air quality becomes increasingly important, relevant studies are rare and mostly focused on the ECAs like the Baltic Sea and the North Sea regions (Jonson et al., 2019; Matthias et al., 2016).

This study aims at understanding the changes in ozone and $PM_{2.5}$ concentrations in Europe in the past as well as estimating the effects of further reductions in land and ship emissions in future. Using the regional chemical transport model CAMx (Comprehensive Air quality Model with eXtensions), we performed simulations for the period between 1990 and 2030 with ten-year intervals and analyzed the temporal and spatial variations in ozone and $PM_{2.5}$ also under different future emission scenarios. In Section 2, all the methods used in this study (model set-up, input preparations, emission scenarios) are described. Section 3 first deals with the changes in emissions in the past and the predicted changes in the future using several emission scenarios. After the model performance evaluation, the main drivers of changes in ozone and $PM_{2.5}$ in the past are discussed. In Section 3.4, the effects of emission changes on ozone and $PM_{2.5}$ are analyzed separately. Finally, the effects of ship emissions are discussed in Section 3.5.

2. Method

The regional air quality model CAMx was used to simulate the air quality in Europe between 1990 and 2030 with ten-year intervals, and to investigate the effects of reduced ship emissions on ozone and $PM_{2.5}$ in the future. The simulations performed in this study can be classified in three groups as follows:

- Base case scenarios in the past for 1990, 2000 and 2010 using the input data for the corresponding years (Table 1).
- Sensitivity scenarios to identify the main drivers (emissions, meteorology, boundary conditions) for the changes in ozone and $PM_{2.5}$ in the past (Table 1).
- Future scenarios with different land and ship emissions for 2020 and 2030 to investigate the role of reduced emissions on trends of ozone and $PM_{2.5}$ in the future (Table 2).

Table 1
Description of the simulations.

Scenarios	Sensitivity	Year of model inputs		
		Meteorology	Boundary conditions	Emission
Base 1990	–	1990	1990	1990
Base 2000		2000	2000	2000
Base 2010		2010	2010	2010
M10B10E00	Emissions	2010	2010	2000
M10B10E90		2010	2010	1990
M00B90E90	Meteorology	2000	1990	1990
M10M90E90		2010	1990	1990
M10B00E00	Boundary conditions	2010	2000	2000
M10B10E00		2010	2010	2000
M10B90E90		2010	1990	1990
M10B10E90		2010	2010	1990

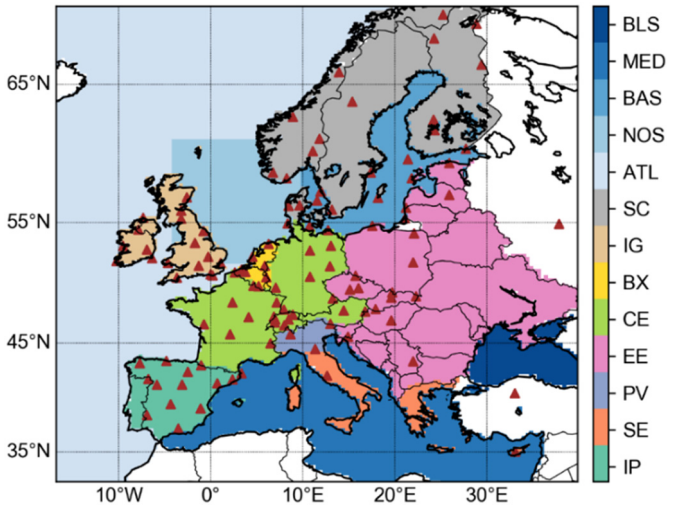

Fig. 1. Model domain and the sub-regions. IP: the Iberian Peninsula, SE: Southern Europe, PV: Po Valley, EE: Eastern Europe, CE: Central Europe, BX: Benelux, IG: Ireland and Great Britain, SC: Scandinavia, ATL: Atlantic Ocean, NOS: North Sea, BAS: Baltic Sea, MED: Mediterranean Sea, BLS: Black Sea. The red triangles indicate 114 EMEP stations in Europe.

2.1. Regional air quality model CAMx

The CAMx version 6.50 (Ramboll, 2018) was used in this study. The domain follows a regular latitude-longitude geographical coordinates with a horizontal resolution of 0.25° and 0.4° which corresponds to about 25 km × 25 km around the central latitudes of the domain. The total coverage extends from 17°W to 39.8°E and from 32°N to 70°N. We divided the model domain into 8 regions on land and 5 sea areas to analyze the model results in specific areas (Fig. 1). There are 14 terrain-following vertical layers ranging from 50 to 8000 m asl. The Carbon Bond 6 Revision 2 (CB6r2) mechanism (Hildebrandt Ruiz and Yarwood, 2013) was used for the gas-phase chemistry. The secondary organic aerosol chemistry/partitioning (SOAP2.1) module was used for the organic aerosol chemistry, which includes recent updates to include the reactions of intermediate volatile organic compound (IVOC) precursors (Ramboll, 2018). Partitioning of inorganic aerosol components was calculated by the ISORROPIA thermodynamic model (Nenes et al., 1998).

The inputs of meteorology and boundary conditions for 1990, 2000 and 2010 were obtained from the EURODELTA-Trends (EDT) project (Colette et al., 2017). The meteorological data in the EDT project was produced by Weather Research and Forecast Model (WRF version 3.3.1) in the EuroCordex domain with a resolution of 0.44°. The dataset was optimized and evaluated by Stegehuis et al. (2015). The meteorological data were re-gridded to our model domain, and further processed by WRFCAMx version 4.4 (http://www.camx.com/download/support-software.aspx) to prepare the meteorological parameters as input for the air quality model CAMx. The initial concentrations of chemical species in each layer of the model domain and at the domain lateral boundaries were based on monthly climatological data (Colette et al., 2017). The ozone column densities were adopted from Total Ozone Mapping Spectrometer (TOMS) data by NASA, and photolysis rates were calculated using the Tropospheric Ultraviolet and Visible (TUV) Radiation Model version 4.8.

Table 2
Description of the land and ship emissions in the future scenarios for 2020 and 2030. Meteorology and boundary conditions of these future scenarios are the same as in 2010.

Scenarios	Ship emissions	Land emissions
2020_CLE	Projected based on current legislation scenario of the ECLIPSE V5a dataset	Projected based on the revised Gothenburg Protocol (2012) relative to 2005
2020_CLEland	Same as 2010 ship emissions	
2030_CLE	Projected based on current legislation scenario of the ECLIPSE V5a dataset	Projected based on the National Emissions Ceilings Directive (2016) relative to 2005
2030_MTFR	Projected based on maximum technically feasible emissions reduction scenario of the ECLIPSE V5a dataset	
2030_CLEland	Same as 2010 ship emissions	

2.2. Emissions

2.2.1. Base case emissions

The anthropogenic emissions of SO_2, NO_x, NH_3, CO, non-methane volatile organic compounds (NMVOC), $PM_{2.5}$ and PM_{coarse} (PM with an aerodynamic diameter between 2.5 and 10 μm) for 1990, 2000 and 2010 were obtained from the EDT database. The emissions from 10 SNAP (Selected Nomenclature for Air Pollution) sectors were based on the annual country total emissions from GAINS (Greenhouse gases and Air pollution Interactions and Synergies), except for NH_3, which were provided by the TNO-MACC (The Netherlands Organization for Applied Scientific Research - Monitoring Atmospheric Composition and Climate) inventory. The NMVOC speciation was conducted following the approach described by Passant (2002). The PM emissions were further split into organic carbon, elemental carbon, sodium, sulfate, and crustal minerals, based on country-specific profiles of TNO (Kuenen et al., 2014). The IVOCs are important precursors of secondary organic aerosol (SOA) (Robinson et al., 2007), but they are absent in the current emission inventories. We estimated the IVOC emissions according to the IVOC/POA factors given in the literature as follows: 4.5 for biomass burning (Ciarelli et al., 2017) and 1.5 for the other anthropogenic sources (Robinson et al., 2007). The biogenic emissions (isoprene, monoterpenes, sesquiterpenes, soil-NO) were generated using the Model of Emissions of Gases and Aerosol from Nature (MEGAN) version 2.1 (Guenther et al., 2012). The anthropogenic emissions were distributed to various vertical layers depending on their sources using the vertical profile given by Bieser et al. (2011). The ship emissions over the sea were separated from SNAP8 and injected to the 2nd model layer. All the biogenic emissions were released to the surface layer.

2.2.2. Future emissions

The anthropogenic emissions for 2020 and 2030 were determined based on current legislations in Europe. Using 2005 as the reference year, the emissions in 2020 and 2030 were calculated by the reduction targets of the revised Gothenburg Protocol (revised on 4 May 2012, https://www.unece.org/env/lrtap/multi_h1.html) and the National Emissions Ceilings (NEC) Directive (2016/2284/EU), respectively. The country-scale emission reduction rates in 2020 and 2030 relative to 2005 are shown in Table S1. A detailed description of the future emission scenarios is given in Table 2. The ship emissions in 2020 and 2030 are projected based on current legislations (CLE) of International Maritime Organization (IMO) and EU (2020_CLE, 2030_CLE). To investigate the maximum potential of ship emission reductions, a maximum technically feasible emission reduction scenario was performed for 2030 (2030_MTFR). Two other scenarios were developed as base scenarios of CLE (2020_CLEland, 2030_CLEland), which adopt the CLE land emissions and keep the ship emissions as in 2010. The reduction rates relative to 2010 in the North Sea, Baltic Sea, Atlantic Sea, Mediterranean Sea, and Black Sea were calculated by the global shipping emissions of the ECLIPSE V5a dataset by the GAINS model (updated in July 2015 by the International Institute for Applied Systems Analysis, IIASA, http://www.iiasa.ac.at/web/home/research/researchPrograms/air/ECLIPSEv5a.html), and used to project emissions by scaling the 2010 ship emissions. For all the future scenarios, meteorology and boundary conditions were kept the same as in 2010.

2.3. Sensitivity tests

Although this study focuses on the effects of emissions on ozone and $PM_{2.5}$, understanding the strength of other drivers is also very important to determine if emissions are the key driving force of the changes. Therefore, some sensitivity tests were performed to investigate the sensitivity of the modeled ozone and $PM_{2.5}$ to the main inputs, i.e. meteorology (M), boundary conditions (B) and emissions (E). Following the sensitivity scenarios of the EDT project (Colette et al., 2017), eight simulations with combinations of inputs from different years were conducted as shown in Table 1 together with the three base case simulations. In order to test the sensitivity to emissions in Europe, we calculated two scenarios with the meteorology and boundary conditions of 2010 and with emissions of 2000 (M10B10E00) and 1990 (M10B10E90), respectively. For sensitivity to meteorological inputs, we performed two simulations with the same boundary conditions and emissions in 1990 but meteorology in 2000 (M00B90E90) and 2010 (M10B90E90). Two additional pairs of scenarios with different boundary conditions were used to test the sensitivity to boundary conditions, i.e. M10B00E00–M10B10E00 and M10B00E90–M10B10E90. The surface-layer model results of each sensitivity scenario were interpolated to 114 EMEP (the co-operative program for the monitoring and evaluation of long-range transmission of air pollutants in Europe) stations (see the spatial distributions in Fig. 1) for further analysis.

2.4. Model evaluation

The model performance was evaluated using measurements in 1990, 2000 and 2010. The measured annual mean concentrations of SO_2, NO_2, PM_{10}, $PM_{2.5}$ and hourly O_3 were obtained from the EDT-project database which are based on the EMEP datasets (https://wiki.met.no/emep/emep-experts/tfmmtrendstations). The number of available measurement stations for each year is presented in Table 3. The statistical metrics for model performance including mean bias (MB), mean error (ME), root-mean-square error (RMSE), mean fractional bias (MFB), mean fractional error (MFE), and Pearson correlation coefficient (r) are given in Table S2. For ozone, only measurements at the background-rural stations were used to reduce uncertainties due to the model resolution.

Table 3
Model performance for annual mean concentrations of chemical species in 1990, 2000 and 2010. MB: mean bias; ME: mean error; RMSE: root-mean-square error; MFB: mean fractional bias; MFE: mean fractional error; r: Pearson correlation coefficient. JJA aft: summer afternoon (June–July–August, 12:00–18:00).

Species	Year	Number of sites	MB[a]	ME[a]	RMSE[a]	MFB (%)	MFE (%)	r
SO_2	1990	38	1.3	1.4	2.3	41.0	49.7	0.77
	2000	52	0.7	0.8	1.0	69.0	79.9	0.85
	2010	49	0.4	0.4	0.6	58.4	67.3	0.78
NO_2	1990	26	1.0	2.1	3.3	6.7	39.2	0.81
	2000	47	1.4	1.8	2.6	23.9	37.1	0.84
	2010	51	0.0	1.2	1.7	−2.2	36.7	0.83
O_3	1990	40	6.7	7.7	9.3	20.5	22.9	0.34
	JJA aft		9.8	9.9	11.8	28.5	28.6	0.73
	2000	64	3.7	5.9	7.1	11.7	17.2	0.50
	JJA aft		5.9	6.9	8.3	19.0	21.3	0.76
	2010	60	5.3	6.5	7.7	16.3	19.2	0.46
	JJA aft		8.8	9.4	11.1	25.4	26.7	0.60
PM_{25}	2000	15	3.5	4.6	6.2	26.1	34.0	0.55
	2010	49	−0.2	2.2	3.3	−1.3	22.6	0.77

[a] Units for gaseous species are ppb, and for particulate species μg m^{-3}.

3. Results and discussion

3.1. Changes in anthropogenic emissions over land and sea

Emissions of major air pollutants from different anthropogenic sources for the whole domain from 1990 to 2030 are shown in Fig. 2. From 1990 to 2010, the largest reduction in Europe occurred in SO_2 emissions (68%) while NH_3 emissions decreased the least (23%). The decrease in emissions of ozone precursors (NMVOC by 55% and NO_x by 36%) as well as in primary $PM_{2.5}$ emissions (by 46%) was quite large. By 2030, the emission reductions compared to 1990 in the model domain will amount to 83% for SO_2, 68% for NMVOC and 68% for $PM_{2.5}$ under current legislation. The energy sector contributes to the largest reduction in SO_2 emissions, while road traffic is the main contributor to the NMVOC and NO_x reductions and the decrease in $PM_{2.5}$ emissions mostly occurs in the industrial process and energy industries. The decrease in most of the emissions slowed down after 2000. The most significant difference is seen for SO_2, for which the emission reduction amounted to 51% from 1990 to 2000 but only to 35% from 2000 to 2010. A similar trend is observed for emissions from residential (non-industrial) combustion. After a mild decrease by ~20% during 1990–2000, the NO_x and NMVOC emissions from the residential sector remained almost unchanged (with a decrease by ~1%) in 2000–2010, and the $PM_{2.5}$ emissions even increased by 4%. After 2010, the NMVOC emissions still declined, however, at a decreased rate (e.g. 33% in 2000–2010 and only 8% in 2020–2030), while the reduction rates for NO_x, SO_2 and $PM_{2.5}$ during 2010–2020 are higher under the revised Gothenburg Protocol compared to 2000–2010. The change in NH_3 emissions is predicted to be smaller than for other species, with a reduction rate of ~7% per decade between 2010 and 2030.

Opposite to the substantial reductions in total anthropogenic land emissions since 1990, the ship emissions continued to increase until 2010 because of increasing international trade as well as a lack of Europe-wide regulations for emissions from shipping activities. The NO_x emissions from ships increased by 53% during 1990–2010, with comparable growth rates during 1990–2000 (26%) and 2000–2010 (21%). The increase in SO_2 emissions over the sea generally slowed down (24% during 1990–2000 compared to 5% during 2000–2010), mostly due to the implementation of the Annex VI of the MARPOL Convention in the Sulfur Emission Control Areas (SECA, the Baltic Sea (entering into force in May 2006), North Sea and the English Channel (entering into force in November 2007)). The $PM_{2.5}$ emissions from ships did not change significantly during 1990–2000, but increased by 9% during 2000–2010. The ship emissions are projected to decrease by 2020 with the implementation of the IMO regulations in Europe, where the SO_2 emissions show the largest decrease (with 84%) from 2010 to 2020, followed by $PM_{2.5}$ (65%) and NO_x (28%). In 2030, ship emissions under the CLE scenario will be kept at the same level as in

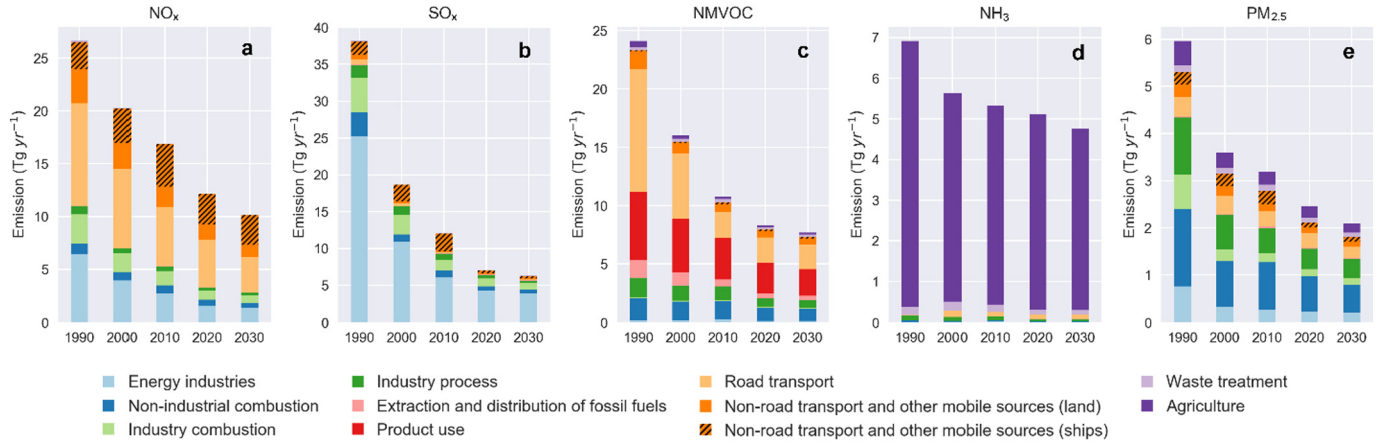

Fig. 2. Changes in emissions of air pollutants from different anthropogenic sources in Europe from 1990 to 2030. Emissions in 2020 and 2030 are based on current legislation (CLE) scenario.

2020, while the MTFR scenario will lead to a further significant decrease in NO_x (76%), SO_2 (64%) and $PM_{2.5}$ (57%) emissions compared to 2020.

3.2. Model performance

The comparison between modeled and measured concentrations of major gaseous and particulate pollutants is shown in Fig. 3 and Table 3. The model evaluation covers the whole period (1990, 2000 and 2010) except for $PM_{2.5}$, which starts at 2000 due to lack of measurements before. The statistical results for summer afternoon (12:00 to 18:00 in June–July–August) ozone are also provided in Table 3 as an indicator of high-level ozone, which is more relevant for impacts on human health and ecosystems than the annual average mixing ratios.

The agreement between the measurements and model results are better in 2010 compared to 1990 most likely due to improvements both in measurements and in model inputs. Overestimation of SO_2 with a mean bias of 1.3 ppb in 1990 is reduced in 2000 and 2010, with a mean bias of 0.7 and 0.4 ppb, respectively. Previous studies also reported a positive bias for SO_2 in Europe (Aksoyoglu et al., 2017; Bessagnet et al., 2016; Ciarelli et al., 2016). The overestimation mainly occurs at sites with high SO_2 emissions especially in the polluted areas in Eastern Europe (Fig. S1). The main reason might be the uncertainties in the vertical distribution of emissions (Bieser et al., 2011). The model injects the emissions into different heights using European average values for stack heights which actually vary with site. In areas with large emission sources and high stacks, application of the average stack heights could cause too high emissions in lower model layers, leading to overestimation of SO_2 mixing ratios. The NO_2 mixing ratios are well predicted, with an MFB ranging from −2% (in 2010) to 24% (2000), which is comparable with reported modeling studies by CAMx

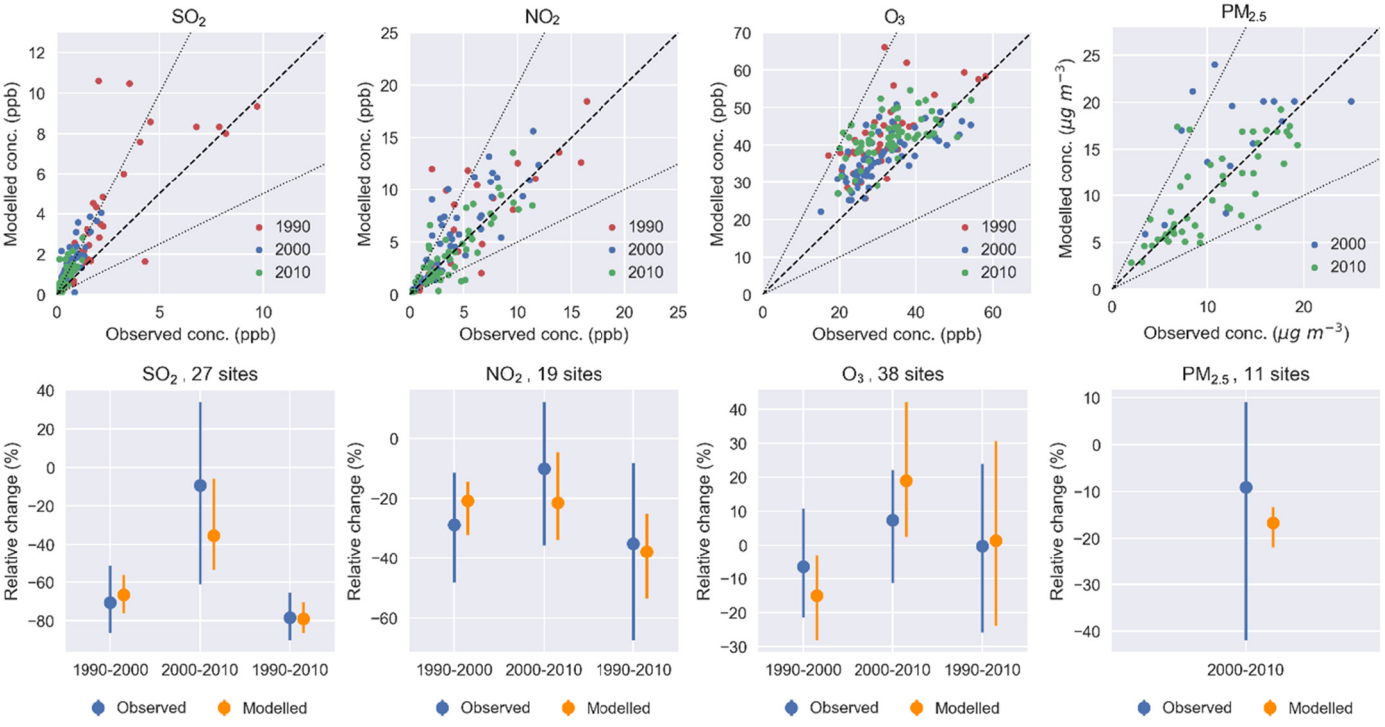

Fig. 3. Comparison of modeled and measured annual mean concentrations (upper panel) for 1990, 2000 and 2010 and relative changes (lower panel) in average concentrations of major air pollutants at a number of EMEP measurement sites. The bars represent the 10th and 90th percentiles of relative changes for all sites. Only summer afternoon (June–July–August, 12:00–18:00) data were used for ozone.

in Europe, such as Oikonomakis et al. (2018a) (MFB = −12%, MFE = 53%), Ciarelli et al. (2016) (MFB = −54% to −28%, MFE = 56% to 68%). Sites in Germany and UK tend to overestimate NO_2 mixing ratios (especially in 2000), while sites in northern Europe and Spain are more likely to underestimate NO_2 (Fig. S1). This may result from the high uncertainty of the NO_x emission inventory (±20% for NO_x compared to 10% for SO_2 according to Kuenen et al. (2014)). In spite of a general overestimation, the ozone mixing ratios still meet the model performance criteria (MFB < ±30%; MFE < 45%) given by EPA (2007). The correlation with observations is relatively low for the annual means while the correlations are much higher for the summer afternoon ozone mixing ratios. The boundary conditions are recognized as the most important reason for the overestimation of ozone. We showed in a previous study, comparing the boundary conditions based on monthly climatological data similar to this study (referred to as EDT boundary conditions) and those from the Model of Ozone and Related Chemical Tracers (MOZART) global model with a time resolution of 6 h (MOZART boundary conditions), that using the EDT boundary conditions as in this study leads to 5–7 ppb higher ozone in western and southern Europe, and 2–3 ppb higher ozone in central Europe than using the MOZART boundary conditions (Aksoyoglu et al., 2019). The modeled $PM_{2.5}$ concentrations are in a good agreement with the measurements, meeting the recommended model performance goal (MFB < ±30%; MFE < 50%) by Boylan and Russell (2006) for both 2000 and 2010.

The modeled and measured changes over time look similar despite some over/underestimations (Fig. 3). As an important precursor of $PM_{2.5}$, the observed SO_2 mixing ratios show a larger decrease during 1990–2000 (70%) than 2000–2010 (10%); the modeled mixing ratios follow a similar trend (1990–2000: 67%, 2000–2010: 36%). The NO_2 measurements also show a stronger decrease during the first decade (29% during 1990–2000, and 10% during 2000–2010), while the modeled NO_2 has a similar decrease (~21%) in both periods. A worse model performance for reproducing the relative change in NO_2 during 2000–2010 compared to 1990–2000 was also reported by other models participating in the EDT project and it was attributed to the effects of coarse resolution on modeling low pollutant concentrations and uncertainties of the measurements (Ciarelli et al., 2019). On the other hand, a recent study suggests that NO_x emissions might be too low in the European emission inventories for 2010 (Oikonomakis et al., 2018a). This could explain the larger NO_2 decrease in the model than in the observations between 2000 and 2010. Both modeled and measured summer afternoon ozone values show a decrease during 1990–2000 and an increase during 2000–2010 (see Section 3.3 for a detailed analysis). The modeled and measured $PM_{2.5}$ values decrease with similar rate (17% and 9%, respectively) during 2000–2010. In spite of significant uncertainties in model inputs and model parameterization, the comparison between modeled and measured trends of air pollutants indicates that the model is capable to capture the changes in ozone and $PM_{2.5}$, as well as to reflect the effects of different emissions.

3.3. Model sensitivity

Besides the anthropogenic emissions, the trends of ozone and $PM_{2.5}$ are also influenced by multiple other factors, such as the meteorological and boundary conditions. Fig. 4 shows the sensitivity analysis results of ozone and $PM_{2.5}$ based on different combination of inputs in 1990, 2000 and 2010. For ozone, the reduced precursor emissions lead to a decrease in high-level ozone values and to an increase in low-level ozone values (Fig. 4a1). The reason for such effects of emissions on ozone mixing ratios will be discussed in Section 3.4.1. The influence of meteorology on ozone does not present a clear pattern (Fig. 4a2). The median ozone values under M90, M00 and M10 (representing the meteorological conditions for 1990, 2000, and 2010, respectively) are quite similar to each other. The different boundary conditions lead to absolute differences of ~1–1.5 ppb for the median ozone (Fig. 4a3), which match with the interannual difference of ozone from the boundaries (Fig. S2).

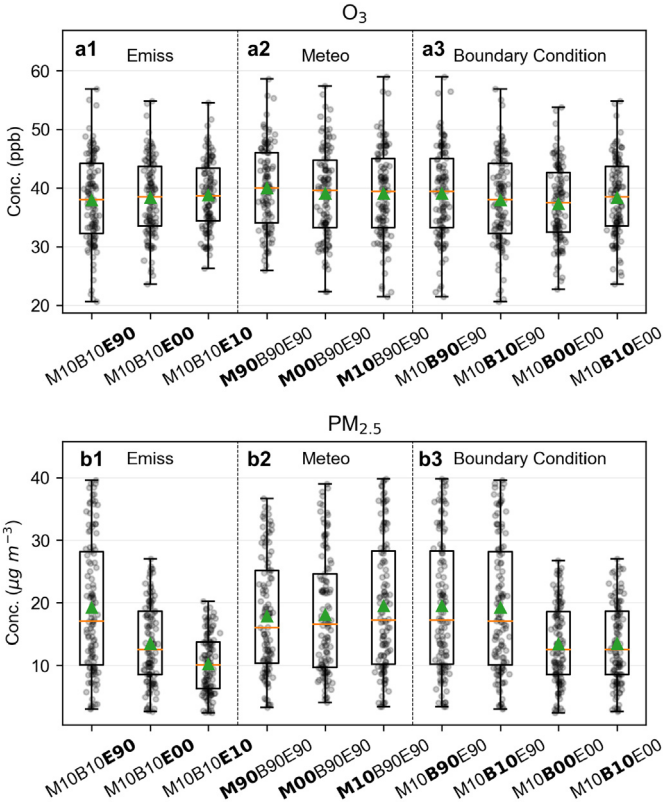

Fig. 4. Influence of emissions, meteorological and boundary conditions on modeled annual mean O_3 (a) and $PM_{2.5}$ (b) concentrations at 114 EMEP stations using different sensitivity scenarios. The orange lines represent median values, and green triangles represent mean values.

The modeled $PM_{2.5}$ values are more sensitive to the changes of inputs compared to ozone. A significant decrease in $PM_{2.5}$ concentrations is found with decreasing emissions from 1990 to 2010 (Fig. 4b1). Benefitting from the reduced emissions of $PM_{2.5}$ and the precursors of aerosols, the modeled mean $PM_{2.5}$ values are 49% lower with 2010 emissions than with 1990 emissions. The effects of meteorology and boundary conditions are much milder than those of the emissions. The modeled median $PM_{2.5}$ values generally increase from M90 to M10, while the modeled surface temperatures at the same stations are higher for M90 than for M10 (Fig. S3). This can be explained by the fact that lower temperatures shift the partitioning of semi-volatile species from the gas phase to the particle phase, resulting in higher concentrations of $PM_{2.5}$. The effects of the boundary conditions on $PM_{2.5}$ (Fig. 4b3) are negligible.

3.4. Trends of ozone and $PM_{2.5}$ between 1990 and 2030

In this section, we present an analysis of the spatial and temporal variations of modeled ozone and $PM_{2.5}$ concentrations from 1990 to 2030. The emission scenarios according to the current legislation (CLE) with reductions in both land and ship emissions were used to represent the air quality in 2020 and 2030, while the meteorology and boundary conditions for 2020 and 2030 were kept the same as in 2010.

3.4.1. Ozone

The spatial distribution of the annual mean ozone mixing ratio in 1990 and the changes in 2000–2030 relative to 1990 are shown in Fig. 5a. During the first decade (1990–2000), annual mean ozone mixing ratios decrease slightly except in the UK and eastern part of the model domain where there is a slight increase. However, with the continuous

decrease in precursor emissions, annual ozone increases continuously in central Europe, UK and Benelux area as well as around the eastern part of the model domain. According to the regional analysis results (Table 4), the regional average ozone increases by 6.3 ppb (22%), 4.2 ppb (8%) and 3.4 ppb (9%) in the Benelux, Central Europe, Ireland & Great Britain, respectively from 1990 to 2030. The annual mean ozone continues to increase from 2000 to 2030 except on the Iberian Peninsula and in southern Europe where it decreases. The increase in the annual mean ozone mixing ratio is especially obvious in polluted, urban areas (i.e. Benelux, Paris and Milan), where ozone production is likely to be more sensitive to VOC emissions (Aksoyoglu et al., 2012). Fig. 5b and c show clearly that the mean ozone mixing ratios increase almost everywhere in winter while the summer mean ozone decreases in a large part of Europe. Consequently, the high ozone levels, which are relevant for impacts on human health and vegetation, decrease during the whole period (see Fig. 5d for the number of days with maximum daily 8-h average ozone (MDA8) exceeding the EU limit of 60 ppb). These numbers are also shown in Table 4 for different European regions. In southern Europe, as well as in the Po Valley and the Iberian Peninsula where MDA8 limit values (60 ppb) are exceeded during half of 1990, the number of exceedance days is reduced by 51% (101 days), 53% (94 days) and 43% (68 days) in 2030, respectively. On the other hand, the smallest change in number of days exceeding the MDA8 limit are predicted in the Benelux area (39 days, 37%) and Ireland & Great Britain (18 days, 22%), where ship emissions influence the air quality significantly (Aksoyoglu et al., 2016).

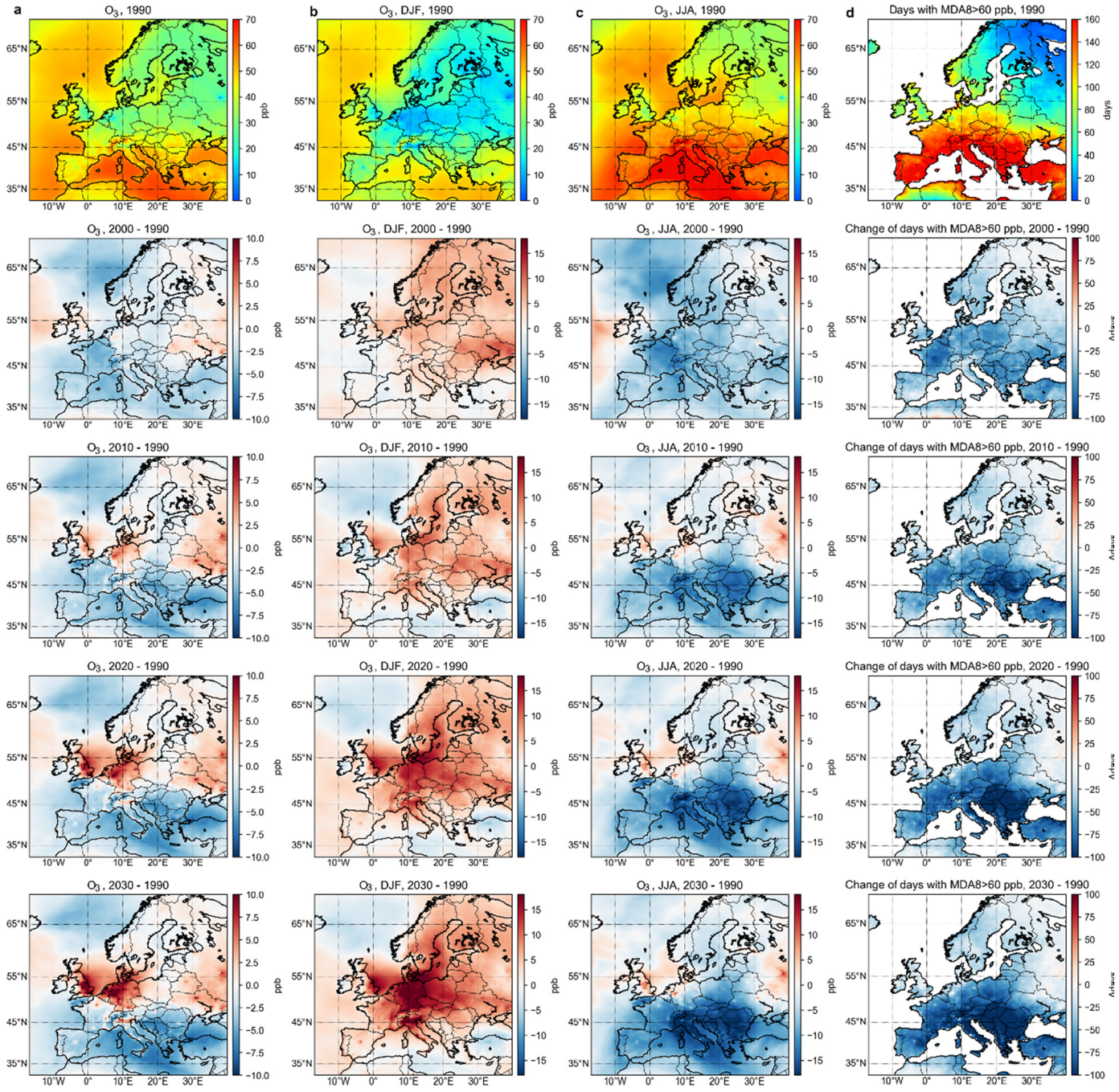

Fig. 5. Changes in (a) annual mean ozone, (b) winter (December–January–February, DJF) mean ozone, (c) summer (June–July–August, JJA) mean ozone and (d) days with maximum daily 8-h average ozone (MDA8) exceeding the EU limits relative to 1990.

Table 4
Regional average of ozone mixing ratios, number of days with maximum daily 8-h average ozone (MDA8) exceeding the EU limits, and $PM_{2.5}$ concentrations from 1990 to 2030.

Species	Year	Iberian Peninsula	Southern Europe	Po Valley	Eastern Europe	Central Europe	Benelux	Ireland & Great Britain	Scandinavia
Ozone (ppb)	1990	46.4	52.0	43.3	37.2	37.9	29.2	37.0	32.3
	2000	43.7	49.4	41.0	36.7	35.2	26.5	37.1	31.2
	2010	44.0	48.7	42.1	36.4	36.8	29.1	37.3	32.3
	2020	43.9	48.2	42.9	36.6	38.3	33.1	39.4	32.7
	2030	43.7	47.7	43.7	36.7	39.2	35.5	40.4	32.7
MDA8 > 60 ppb (days)	1990	158	197	177	107	135	106	85	44
	2000	125	157	151	58	80	47	66	21
	2010	118	142	126	54	82	67	65	24
	2020	105	118	109	43	71	68	66	23
	2030	90	96	82	39	62	67	66	22
$PM_{2.5}$ ($\mu g\ m^{-3}$)	1990	10.4	14.7	25.2	23.5	26.0	29.2	12.8	5.9
	2000	8.2	10.1	17.1	14.5	17.3	20.6	9.1	5.3
	2010	5.7	7.3	12.5	12.8	13.7	17.3	8.6	4.1
	2020	4.3	5.4	8.7	10.1	9.7	12.4	6.3	3.2
	2030	3.5	4.7	6.5	8.7	7.2	9.7	5.0	3.0

The distinct trends for the high-level and low-level ozone agree with previous studies in Europe (Jonson et al., 2006; Yan et al., 2018). The high-level ozone occurs in summer, when high temperatures largely enhance the photochemistry for ozone production which dominates the ozone levels. Therefore, reduced precursor emissions bring down the high-level ozone. However, for the low-level ozone in winter, when the ozone production is limited by lower temperatures, the destruction of ozone by NO titration becomes more important. The decreased NO_x emissions lead to less ozone titration with NO and therefore cause an increase in the low-level ozone, especially in urban areas with high NO_x emissions such as the Benelux region (Fig. 5b). As shown in Fig. S4, there is almost no spatial variance in winter Ox ($O_3 + NO_2$) in these areas and they look very similar in 1990, 2000 and 2010, suggesting that the increase in ozone was mainly caused by less titration (Clapp and Jenkin, 2001) as a result of reduced emissions. The effect of increased surface solar radiation (SSR) between 1990 and 2010 on mean ozone was predicted to be very small (Oikonomakis et al., 2018b).

The model results for future scenarios indicate that the trend will be largely enhanced under current emission reduction legislations. Between 1990 and 2010, the mean ratio of VOC/NO_x emissions in Europe (except for some urban areas) decreases as a result of larger reductions in VOC emissions compared to NO_x (Fig. S5a, c). The situation changes after 2010 when the ratio of VOC/NO_x emissions starts to increase due to more strict NO_x emission reductions (Fig. S5d). Although the number of days with MDA8 exceeding the EU limit is predicted to decrease further by 2030, the EU standard of 25 days of exceedance per year still cannot be reached in most of Europe.

3.4.2. $PM_{2.5}$

$PM_{2.5}$ concentrations significantly decrease during the period of 1990–2030 (Fig. 6). The domain average $PM_{2.5}$ concentrations decrease from 11.2 $\mu g\ m^{-3}$ in 1990 to 4.9 $\mu g\ m^{-3}$ in 2030 (−56%). The largest absolute decrease during this time period is seen in the Benelux (−29.2 $\mu g\ m^{-3}$, −69%), central Europe (−26.0 $\mu g\ m^{-3}$, −72%) and the Po Valley region (−25.2 $\mu g\ m^{-3}$, −74%). The area with highest $PM_{2.5}$ concentrations generally shifts from central Europe in 1990 to eastern Europe in 2030. The spatial distribution of $PM_{2.5}$ concentrations in 2030 indicates that the emissions around the eastern part of the domain becomes more important for the $PM_{2.5}$ levels (Fig. 6e). With decreasing $PM_{2.5}$ concentrations, the area exposed to $PM_{2.5}$ exceeding the WHO air quality guidelines (AQG) of 10 $\mu g\ m^{-3}$ will also decrease significantly. In 1990, about 63% of the land area have $PM_{2.5} > 10\ \mu g\ m^{-3}$, while this number drops to 40% in 2010, 23% in 2020 and 10% in 2030 (mostly in Benelux and western Russia).

The concentrations of $PM_{2.5}$ components show also significant changes over Europe between 1990 and 2030 (Fig. 7). Sulfate (PSO_4) contributes most to the domain average $PM_{2.5}$ concentrations for the whole period, followed by particulate nitrate (PNO_3) and ammonium (PNH_4). The contribution of each component to the decrease in domain average $PM_{2.5}$ concentrations varies strongly with time. After a substantial drop in the first decade (1990–2000), there is a relatively slow decrease for most of the components. In the first decade (1990–2000), PSO_4, PNH_4 and fine primary material (FPRM) contribute most to the decrease in $PM_{2.5}$ concentrations with fractions of 44%, 15% and 14%, respectively, to total reduction. The contribution of PNO_3 to the decrease in $PM_{2.5}$ concentrations increases later, with 22% in 2000–2010 and 36% in 2020–2030. From 1990 to 2030, FPRM, PSO_4, anthropogenic secondary organic aerosol (SOAa) and PNH_4 show a higher reduction rate than total $PM_{2.5}$ (−56.4%), while primary organic aerosol (POA), elemental carbon (PEC), and PNO_3 follow a reduction rate similar to total $PM_{2.5}$, and the reduction of other components are much slower than total $PM_{2.5}$. As a consequence, the projected relative fractions of $PM_{2.5}$ components present a decrease between 1990 and 2030 in PSO_4 (from 31% to 21%) and in PNH_4 (from 13% to 10%) while the fraction of PNO_3 is predicted to increase slightly (from 19% to 20%). A slight increase is also predicted in the fractions of other components such as biogenic SOA (bSOA), fine crustal (FCRS), sodium (NA) and chloride (PCL).

3.5. Effects of ship emissions on ozone and $PM_{2.5}$

To investigate the effects of changes in ship emissions on ozone and $PM_{2.5}$ concentrations, we compared future scenarios without and with ship emission controls in 2020 and 2030. The baseline scenarios use ship emissions of 2010 (CLEland), while the other two scenarios CLE (current legislation) and MTFR (maximum technically feasible reduction) consider both the increase in international shipping and implementation of different emission control policies which mainly focus on SO_2, NO_x, and $PM_{2.5}$ emissions. The differences between different ship emission scenarios are displayed in Fig. S6. Emissions of all species in each future scenario are lower in the Mediterranean and the area covering the English Channel, North Sea and Baltic Sea compared to the baseline scenario (CLEland) in which the ship emissions are kept the same as in 2010. On the other hand, along the Atlantic coast between southern Spain and the English Channel, NMVOC emissions are higher in all future scenarios. In the same region also NO_x emissions increase in 2020 and 2030 according to the CLE scenarios. These results suggest that only with MTFR scenario a decrease in NO_x emissions can be obtained along the Atlantic coast. The $PM_{2.5}$ emissions from ships using the MTFR scenario are about 64% lower than those with the CLE scenario in 2030, whereas NO_x and SO_2 emissions in MTFR are about 20%–30% lower than in CLE in the Emission Control Areas (i.e. North Sea and Baltic Sea) and ~80% lower in the Mediterranean Sea, Black Sea and the Atlantic.

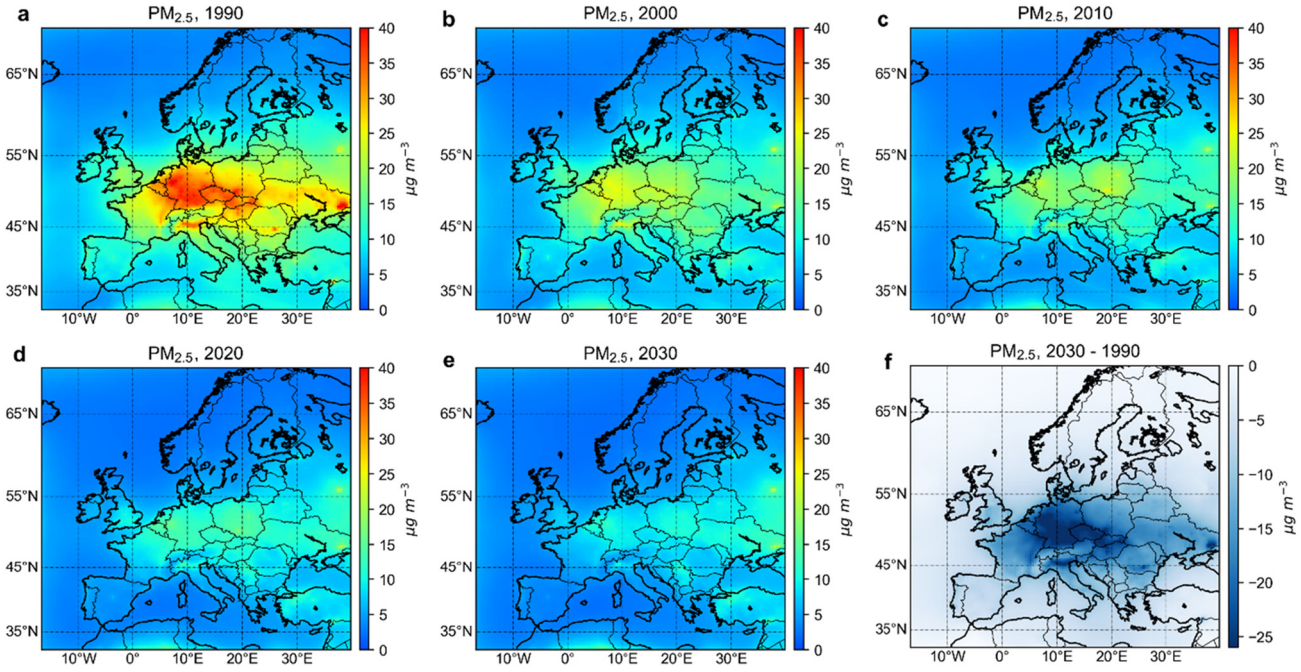

Fig. 6. Annual mean concentrations of $PM_{2.5}$ from 1990 to 2030 (a–e) and absolute changes in 2030 relative to 1990 (f).

3.5.1. Ozone

The effects of different ship emission scenarios on ozone mixing ratios are shown in Fig. 8. Compared to the baseline scenarios keeping the ship emissions the same as in 2010, the current legislation scenario (CLE) leads to an increase in annual mean ozone in 2020 and 2030 at all coastal areas, except around the English Channel. Only with MTFR a decrease in the Mediterranean can be obtained (except along the ship tracks). The regional analysis results (Table S4) show that the average ozone over the North Sea for CLE is higher than for the baseline scenario (CLEland) by ~0.9 ppb (2%). The increase in ozone mostly occurs along the ship tracks, due to the reduced ozone titration with NO with decreased NO_x emissions. An exception is the English Channel, where the annual ozone decreases under CLE, as there are probably still sufficiently large NO_x emissions in that small area with a lot of ship traffic, leading to titration of ozone. A similar result was also reported by Matthias et al. (2016), showing that ozone in the English Channel decreased with mild NO_x reductions and increased when more strict rules for NO_x reduction were applied.

The different ship emissions also affect ozone over the land area differently (Fig. 8). In winter, the CLE and MTFR scenarios in 2030 lead to a small increase over the land (~0.1 ppb for the domain average, and up to 1.2 ppb in the Benelux region) compared to the baseline scenario (CLEland), as the reduced NO_x emissions from ships lower the destruction of ozone by NO titration. In summer, the CLE ship emissions cause an average decrease in ozone over the land area within the domain by 0.2 ppb and 0.1 ppb in 2020 and 2030, respectively. The largest effect

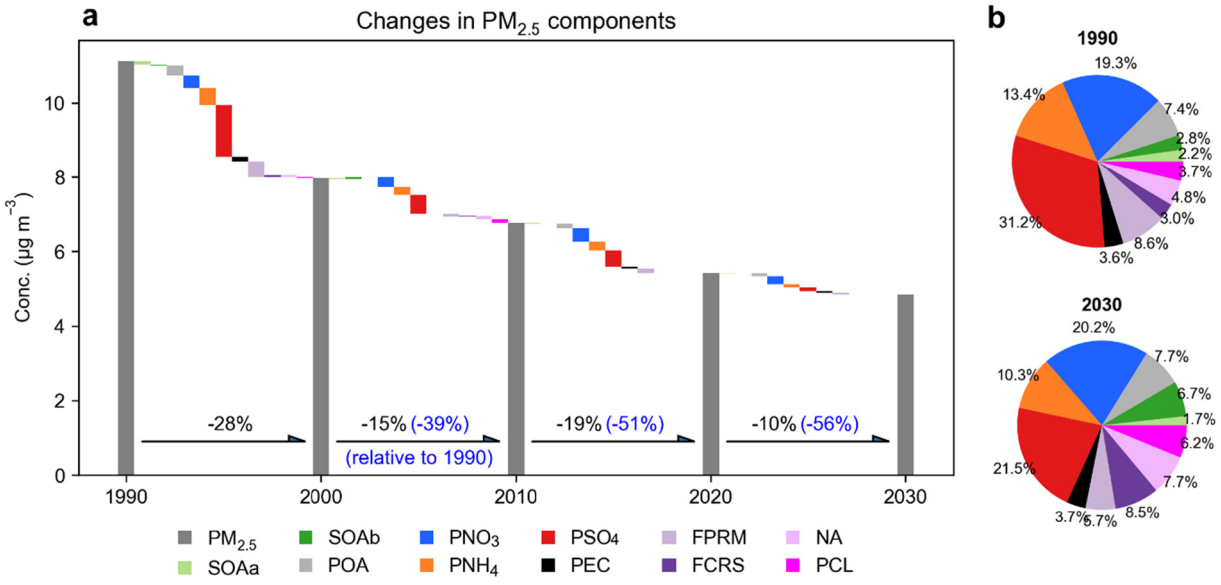

Fig. 7. Annual mean concentrations (a) and relative contributions (b) of $PM_{2.5}$ components between 1990 and 2030. See Table S3 for concentrations of each component from 1990 to 2030. SOAa: anthropogenic secondary organic aerosol SOA, SOAb: biogenic SOA, POA: primary organic aerosol, PNO_3: particulate nitrate, PNH_4: ammonium, PSO_4: sulfate, PEC, elemental carbon, FPRM: fine primary material, FCRS: fine crustal, NA: sodium, PCL: chloride.

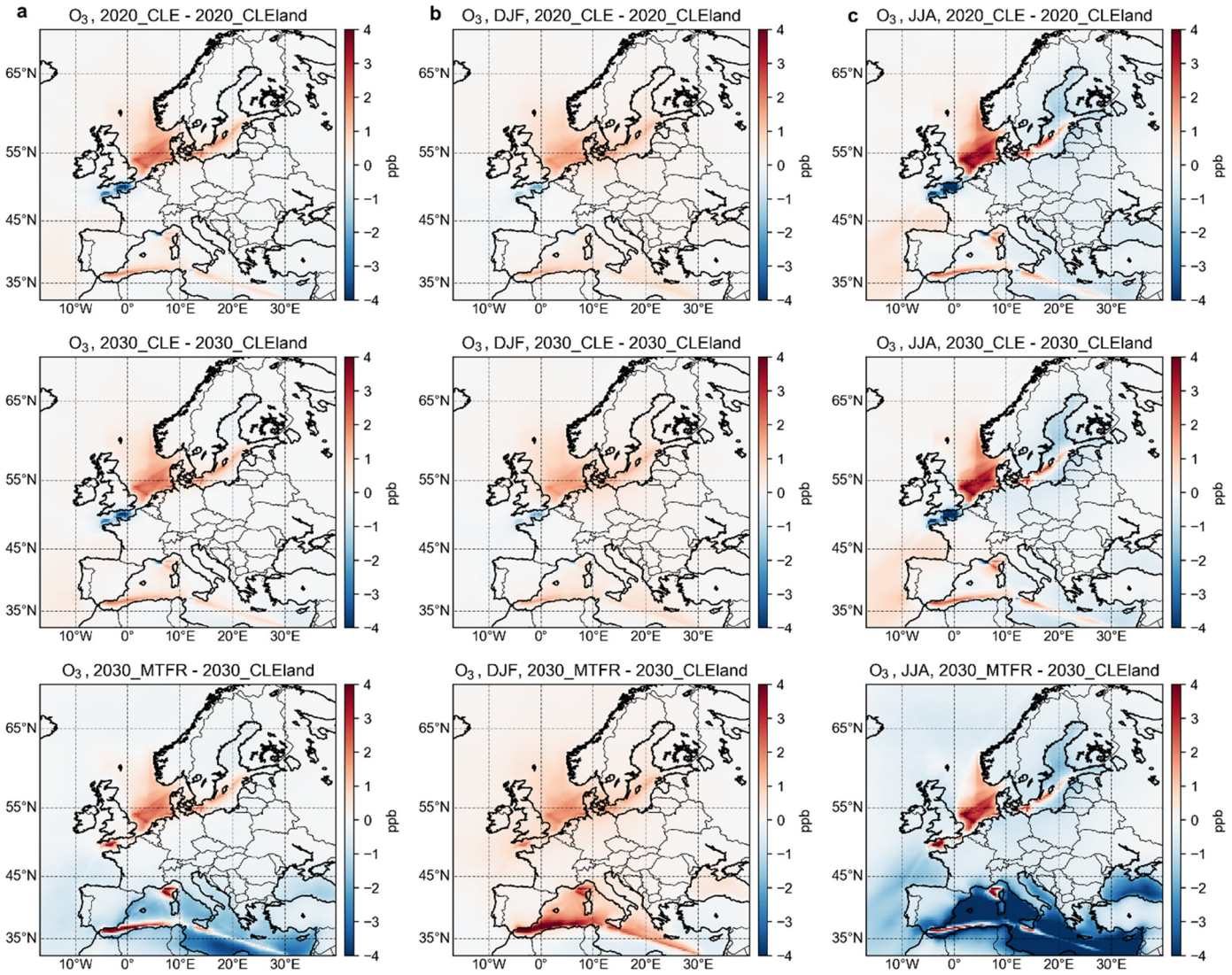

Fig. 8. Effects of different ship emission scenarios on (a) annual mean, (b) winter (DJF: December–January–February) and (c) summer (JJA: June–July–August) ozone mixing ratios. CLEland: with ship emissions of 2010; CLE: with ship emissions under current legislation; MTFR: with ship emissions under maximum technically feasible reductions.

occurs around the English Channel, where a maximum decrease of ~3 ppb is found in a grid-scale. The largest decrease in ozone levels over land reaches 8 ppb (in a grid-scale) around southern Spain and North Africa with the MTFR scenario. The decrease in summer ozone with the CLE scenario leads to a decrease in the number of days (~2 days on average for Europe, and up to 17 days for 2020 and 14 days for 2030 for a grid-scale) with MDA8 higher than 60 ppb compared to the baseline in most regions on land, except in Spain and France where it is influenced by the increase in VOC and NO_x emissions in the Atlantic Sea. In the MTFR case, the days with MDA8 exceeding the EU limit decrease by 6 days on average for whole Europe reaching a maximum reduction of 97 days around southern Spain compared to the base case. The reduced ship emissions under MTFR contribute more than 20% of the total decrease of days with MDA8 exceeding the EU limit relative to 2010 in regions close to the ocean (29%, 1 day in Scandinavia, 27%, 10 days in the Iberian Peninsula, 24%, 14 days in Southern Europe), and ~ 10% for the inland regions (11%, 5 days in Po Valley, ~10%, 2 days in central and eastern Europe) (Fig. 9).

3.5.2. $PM_{2.5}$

The effects of ship emissions on $PM_{2.5}$ are more obvious than those on ozone (Fig. 10, Table S4). The $PM_{2.5}$ concentrations over the sea and coastal areas decrease significantly with the reduction of ship emissions. The largest decrease is predicted over the Mediterranean Sea, where the regional average $PM_{2.5}$ concentrations with CLE and MTFR scenarios are ~14% and ~ 19% lower than those in the base case, respectively. Using the CLE scenario, the largest decrease over land is predicted in the Benelux area (−6% and 0.8 μg m^{-3} in 2020, −7% and 0.8 μg m^{-3} in 2030), while the highest absolute reduction by 1.2 μg m^{-3} (11%) is achieved in the Benelux with the MTFR scenario. The decrease in $PM_{2.5}$ concentrations (compared to the baseline) due to reduced ship emissions (CLE) in 2020 is between 6% (Po Valley) and 18% (Scandinavia) of the total change in $PM_{2.5}$ during the period of 2010–2020. The contribution of ship emission reductions to the $PM_{2.5}$ concentration over land slightly decreases in 2030 (relative to 2010) under CLE (4%–15%) with the enhanced land emission reductions, but will increase to the same level as 2010–2020 under the MTFR scenario (Fig. 9).

We also investigated the effects of changes in ship emissions on the main $PM_{2.5}$ components (PSO_4, PNO_3 and PNH_4). Among all the $PM_{2.5}$ components, the reduction of ship emissions contributes most to the decrease of sulfate on average, with a maximum fraction of 32% in the Iberian Peninsula under MTFR (Fig. S7). The contributions of different $PM_{2.5}$ components to the decreased $PM_{2.5}$ concentrations show a large spatial variation (Fig. 10). In the Mediterranean region, the decrease in

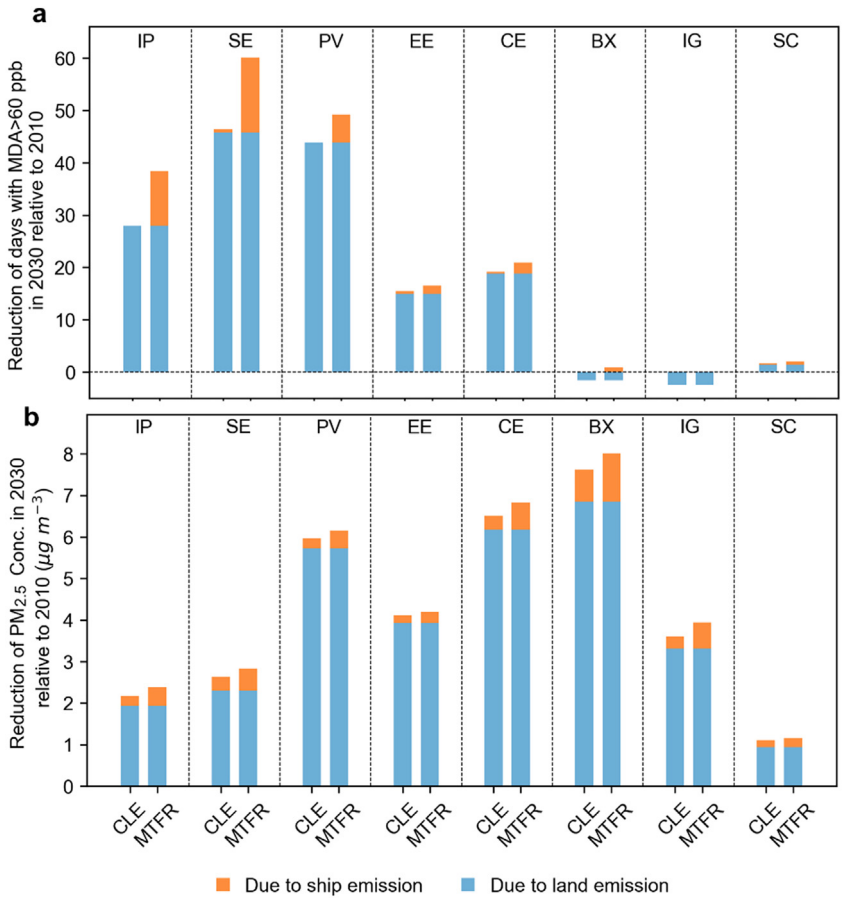

Fig. 9. Contribution of reduced land and ship emissions to the change in days of MDA8 (for ozone) exceeding the EU limit (a) and to the change in $PM_{2.5}$ (b) in different European regions in 2030 relative to 2010.

$PM_{2.5}$ mostly comes from the decrease in PSO_4, benefiting from the reduction of SO_2 emissions from ships under CLE and MTFR scenarios. The regional average contribution of decreased PSO_4 to the $PM_{2.5}$ reduction is about 69% in the Mediterranean Sea and 77% in Iberian Peninsula. In the Benelux and the UK, the reduced NO_x emissions in the North Sea contribute most to the $PM_{2.5}$ reductions. The ratio of decreased PNO_3 to decreased $PM_{2.5}$ is about 49% under CLE scenario and increases to 56% with the MTFR scenario in 2030.

4. Conclusions

The European air quality between 1990 and 2030 was modeled with ten-year intervals with the regional air quality model CAMx, and the results were analyzed in 13 different land and sea regions. The objective of this study was on the one hand to identify the main drivers leading to changes in ozone and fine particulate matter ($PM_{2.5}$) and its components in the past (1990–2010), on the other hand to predict their concentrations in the future (2020−2030) based on different land and ship emission scenarios. The model results suggest that the emissions were the main drivers for the changes in $PM_{2.5}$ concentrations between 1990 and 2010 while meteorology and boundary conditions had negligible effects. On the other hand, changes in ozone were too small to define the drivers clearly. Mean ozone levels decreased slightly during the first decade but then started increasing again especially in polluted areas. Results from the future scenarios suggest that by 2030, the peak ozone will decrease, leading to a decrease in the regional average number of days exceeding the maximum daily 8-h average ozone limit values (60 ppb) by 51% (101 days), 53% (94 days) and 43% (68 days) in southern Europe, the Po Valley and the Iberian Peninsula, respectively, relative to 1990. In the past between 1990 and 2000, the modeled average $PM_{2.5}$ concentrations decreased by 56% (largest decrease by 74% in Po Valley), mostly due to a large drop in sulfate (up to 44% of total $PM_{2.5}$ reduction during 1990–2000) while the contribution from nitrate reduction becomes increasingly important (36% of total $PM_{2.5}$ reduction during 2020–2030).

While land emissions have been decreasing substantially due to large efforts in Europe, emissions from international shipping activities have been increasing since 1990 although some regulations have started in the emission control areas such as SECA (Baltic Sea and North Sea) and at some ports. Adverse effects of ship emissions on air quality are especially attracting attention in the Mediterranean for which there has been no similar regulation yet as in northern Europe. Using the current legislation (CLE) and maximum technically feasible reduction (MTFR) scenarios for the future, we predicted a general increase in ozone over the sea due to reductions in ship emissions (mainly NO_x), except for the English Channel where ozone will decrease. Over the land, high ozone levels will decrease under the CLE scenario, by as much as ~8 ppb (in a grid-scale) around southern Spain and North Africa with the MTFR scenario in 2030. For regions close to the sea, the reduced ship emissions under MTFR will be responsible for 24% to 28% (10 to 14 days) of the total regional average reduction of days of MDA8 exceeding EU limits and to contribute up to 19% (1.2 μg m^{-3} for absolute change) to the decrease in $PM_{2.5}$ concentrations from 2010 to 2030.

Our study suggests that emissions are the main drivers for changes in $PM_{2.5}$ concentrations while it is more difficult to achieve a fast and significant decrease in ozone levels. Although the high-level ozone indicator MDA8 is predicted to further decrease with the reduced land and ship emissions in Europe, the EU standard of 25 days of MDA8 exceedance per year still cannot be reached in most of Europe. Further studies are needed to investigate the effects from multiple factors such as climate

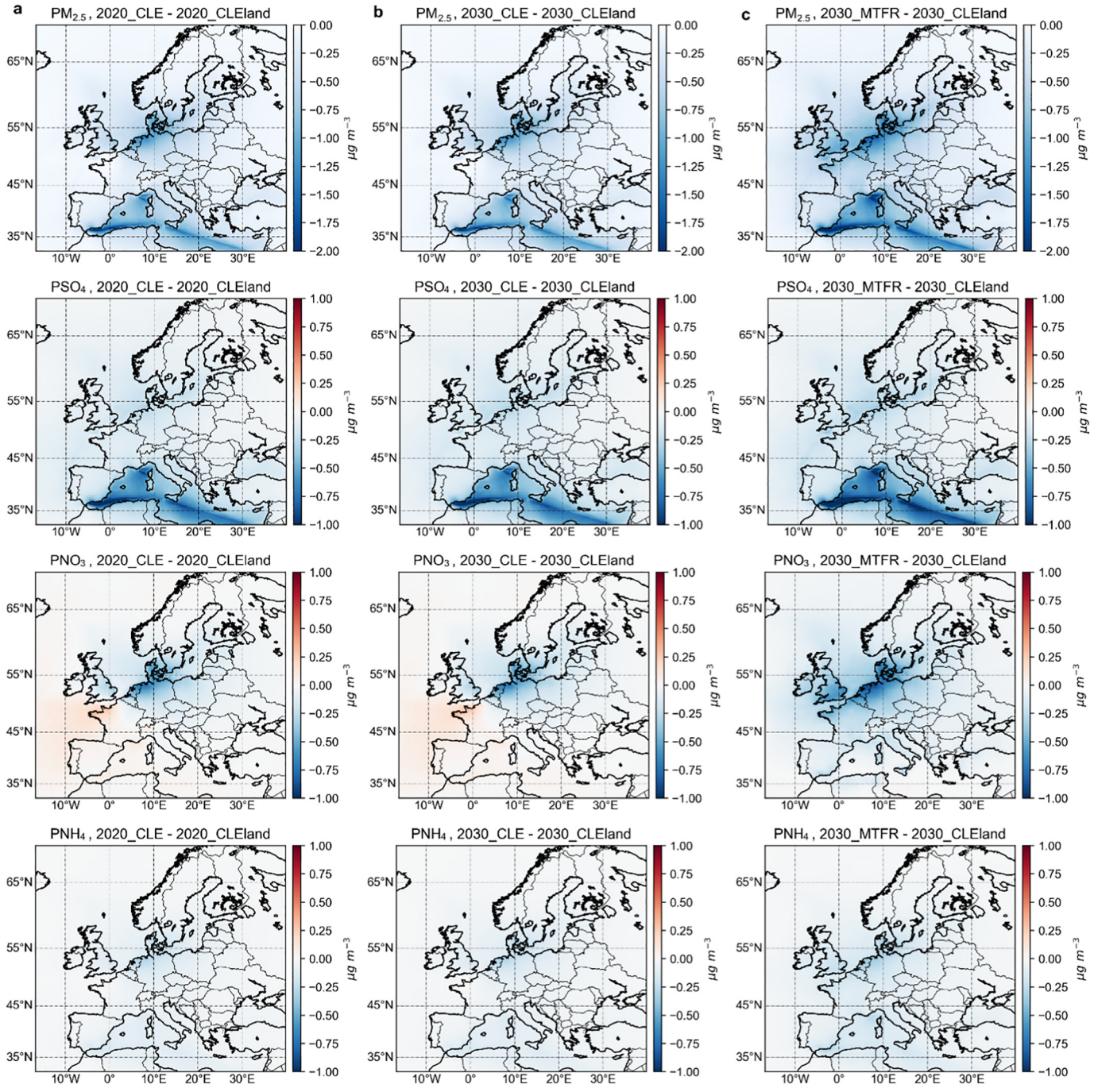

Fig. 10. Effects of different ship emission scenarios on $PM_{2.5}$ and the main $PM_{2.5}$ components. CLEland: with ship emissions of 2010; CLE: with ship emissions under current legislation; MTFR: with ship emissions under maximum technically feasible reductions.

change and intercontinental transport. The results obtained in our study also show the increasing importance of ship emission reductions in the next few decades, after a large decrease in land emissions has been achieved generally in Europe. Further research based on more specific ship emission reduction techniques and covering a larger area of the world will contribute to more effective ship emission control strategies in the future.

CRediT authorship contribution statement

Jianhui Jiang: Conceptualization, Methodology, Formal analysis, Writing - original draft.**Sebnem Aksoyoglu:**Conceptualization, Project administration, Writing - review & editing.**Giancarlo Ciarelli:**Resources, Writing - review & editing.**Urs Baltensperger:**Supervision, Writing - review & editing.**André S.H. Prévôt:**Supervision, Writing - review & editing.

Declaration of competing interest

The authors declare that they have no known competing financial interests or personal relationships that could have appeared to influence the work reported in this paper.

Acknowledgement

This study was financially supported by the Swiss Federal Office for the Environment (FOEN, contract no. 16.0096 PJ/Q233-1014). We

would like to thank RAMBOLL for support in CAMx modeling. We acknowledge the EURODELTA-Trends project for providing meteorological data, anthropogenic emissions and boundary conditions as model input for 1990–2010, the National Aeronautics and Space Administration (NASA) and its data-contributing agencies (NCAR, UCAR) for the TOMS and MODIS data and the TUV model, the International Institute for Applied Systems Analysis (IIASA) for the GAINS ship emissions in 2020 and 2030. Simulation of CAMx model was performed at the Swiss National Supercomputing Centre (CSCS). Giancarlo Ciarelli acknowledges the support of the Swiss National Science Foundation (grant no. P2EZP2_175166).

Appendix A. Supplementary data

Supplementary data to this article can be found online at https://doi.org/10.1016/j.scitotenv.2020.140467.

References

Aksoyoglu, S., Keller, J., Oderbolz, D.C., Barmpadimos, I., Prévôt, A.S.H., Baltensperger, U., 2012. Sensitivity of ozone and aerosols to precursor emissions in Europe. Int. J. Environ. Pollut. 50, 451–459. https://doi.org/10.1504/ijep.2012.051215.

Aksoyoglu, S., Keller, J., Ciarelli, G., Prévôt, A.S.H., Baltensperger, U., 2014. A model study on changes of European and Swiss particulate matter, ozone and nitrogen deposition between 1990 and 2020 due to the revised Gothenburg protocol. Atmos. Chem. Phys. 14, 13081–13095. https://doi.org/10.5194/acp-14-13081-2014.

Aksoyoglu, S., Baltensperger, U., Prévôt, A.S.H., 2016. Contribution of ship emissions to the concentration and deposition of air pollutants in Europe. Atmos. Chem. Phys. 16, 1895–1906. https://doi.org/10.5194/acp-16-1895-2016.

Aksoyoglu, S., Ciarelli, G., El-Haddad, I., Baltensperger, U., Prévôt, A.S.H., 2017. Secondary inorganic aerosols in Europe: sources and the significant influence of biogenic VOC emissions, especially on ammonium nitrate. Atmos. Chem. Phys. 17, 7757–7773. https://doi.org/10.5194/acp-17-7757-2017.

Aksoyoglu, S., Jiang, J., Oikonomakis, E., Prévôt, A.S.H., 2019. Same model (CAMx6.50), same year (2010), two different European projects: how similar are the results? ITM 2019 - 37th International Technical Meeting on Air Pollution Modelling and its Application, Hamburg

Aulinger, A., Matthias, V., Zeretzke, M., Bieser, J., Quante, M., Backes, A., 2016. The impact of shipping emissions on air pollution in the greater North Sea region – part 1: current emissions and concentrations. Atmos. Chem. Phys. 16, 739–758. https://doi.org/10.5194/acp-16-739-2016.

Barna, M., Lamb, B., Westberg, H., 2001. Modeling the effects of VOC/NOx emissions on ozone synthesis in the Cascadia airshed of the Pacific Northwest. J. Air Waste Manage. Assoc. 51, 1021–1034. https://doi.org/10.1080/10473289.2001.10464330.

Bessagnet, B., Pirovano, G., Mircea, M., Cuvelier, C., Aulinger, A., Calori, G., Ciarelli, G., Manders, A., Stern, R., Tsyro, S., Vivanco, M.G., Thunis, P., Pay, M.T., Colette, A., Couvidat, F., Meleux, F., Rouil, L., Ung, A., Aksoyoglu, S., Baldasano, J.M., Bieser, J., Briganti, G., Cappelletti, A., D'Isidoro, M., Finardi, S., Kranenburg, R., Silibello, C., Carnevale, C., Aas, W., Dupont, J.C., Fagerli, H., Gonzalez, L., Menut, L., Prévôt, A.S.H., Roberts, P., White, L., 2016. Presentation of the EURODELTA III intercomparison exercise - evaluation of the chemistry transport models' performance on criteria pollutants and joint analysis with meteorology. Atmos. Chem. Phys. 16, 12667–12701. https://doi.org/10.5194/acp-16-12667-2016.

Bieser, J., Aulinger, A., Matthias, V., Quante, M., Denier van der Gon, H.A.C., 2011. Vertical emission profiles for Europe based on plume rise calculations. Environ. Pollut. 159, 2935–2946. https://doi.org/10.1016/j.envpol.2011.04.030.

Boylan, J.W., Russell, A.G., 2006. PM and light extinction model performance metrics, goals, and criteria for three-dimensional air quality models. Atmos. Environ. 40, 4946–4959. https://doi.org/10.1016/j.atmosenv.2005.09.087.

Chen, D.S., Tian, X.L., Lang, J.L., Zhou, Y., Li, Y., Guo, X.R., Wang, W.L., Liu, B., 2019. The impact of ship emissions on $PM_{2.5}$ and the deposition of nitrogen and sulfur in Yangtze River Delta, China. Sci. Total Environ. 649, 1609–1619. https://doi.org/10.1016/j.scitotenv.2018.08.313.

Ciarelli, G., Aksoyoglu, S., Crippa, M., Jimenez, J.L., Nemitz, E., Sellegri, K., Äijälä, M., Carbone, S., Mohr, C., O'Dowd, C., Poulain, L., Baltensperger, U., Prévôt, A.S.H., 2016. Evaluation of European air quality modelled by CAMx including the volatility basis set scheme. Atmos. Chem. Phys. 2016, 10313–10332. https://doi.org/10.5194/acpd-15-35645-2015.

Ciarelli, G., Aksoyoglu, S., El Haddad, I., Bruns, E.A., Crippa, M., Poulain, L., Äijälä, M., Carbone, S., Freney, E., O'Dowd, C., Baltensperger, U., Prévôt, A.S.H., 2017. Modelling winter organic aerosol at the European scale with CAMx: evaluation and source apportionment with a VBS parameterization based on novel wood burning smog chamber experiments. Atmos. Chem. Phys. 17, 7653–7669. https://doi.org/10.5194/acp-17-7653-2017.

Ciarelli, G., Theobald, M.R., Vivanco, M.G., Beekmann, M., Aas, W., Andersson, C., Bergström, R., Manders-Groot, A., Couvidat, F., Mircea, M., Tsyro, S., Fagerli, H., Mar, K., Raffort, V., Roustan, Y., Pay, M.T., Schaap, M., Kranenburg, R., Adani, M., Briganti, G., Cappelletti, A., D'Isidoro, M., Cuvelier, C., Cholakian, A., Bessagnet, B., Wind, P., Colette, A., 2019. Trends of inorganic and organic aerosols and precursor gases in Europe: insights from the EURODELTA multi-model experiment over the 1990–2010 period. Geosci. Model Dev. 12, 4923–4954. https://doi.org/10.5194/gmd-12-4923-2019.

Clapp, L.J., Jenkin, M.E., 2001. Analysis of the relationship between ambient levels of O_3, NO_2 and NO as a function of NO chi in the UK. Atmos. Environ. 35, 6391–6405. https://doi.org/10.1016/s1352-2310(01)00378-8.

Colette, A., Andersson, C., Manders, A., Mar, K., Mircea, M., Pay, M.T., Raffort, V., Tsyro, S., Cuvelier, C., Adani, M., Bessagnet, B., Bergström, R., Briganti, G., Butler, T., Cappelletti, A., Couvidat, F., D'Isidoro, M., Doumbia, T., Fagerli, H., Granier, C., Heyes, C., Klimont, Z., Ojha, N., Otero, N., Schaap, M., Sindelarova, K., Stegehuis, A.I., Roustan, Y., Vautard, R., van Meijgaard, E., Vivanco, M.G., Wind, P., 2017. EURODELTA-trends, a multi-model experiment of air quality hindcast in Europe over 1990–2010. Geosci. Model Dev. 10, 3255–3276. https://doi.org/10.5194/gmd-10-3255-2017.

Crippa, M., Janssens-Maenhout, G., Dentener, F., Guizzardi, D., Sindelarova, K., Muntean, M., Van Dingenen, R., Granier, C., 2016. Forty years of improvements in European air quality: regional policy-industry interactions with global impacts. Atmos. Chem. Phys. 16, 3825–3841. https://doi.org/10.5194/acp-16-3825-2016.

EEA, 2013. The Impact of International Shipping on European Air Quality and Climate Forcing. European Environment Agency, Luxembourg.

EEA, 2019a. Air Quality in Europe - 2019 Report. European Environment Agency, Luxembourg.

EEA, 2019b. European Uniion Emission Inventory Report 1990–2017 under the UNECE Convention on Long-Range Transboundary Air Pollution (LRTAP). European Environment Agency, Copenhagen, Denmark.

EPA, 2007. Guidance on the Use of Models and Other Analyses for Demonstrating Attainment of Air Quality Goals for Ozone, $PM_{2.5}$, and Regional Haze. U.S. Environmental Protection Agency, Office of Air Quality Planning and Standards, Research Triangle Park, North Carolina.

Guenther, A.B., Jiang, X., Heald, C.L., Sakulyanontvittaya, T., Duhl, T., Emmons, L.K., Wang, X., 2012. The model of emissions of gases and aerosols from nature version 2.1 (MEGAN2.1): an extended and updated framework for modeling biogenic emissions. Geosci. Model Dev. 5, 1471–1492. https://doi.org/10.5194/gmd-5-1471-2012.

Guerreiro, C.B.B., Foltescu, V., de Leeuw, F., 2014. Air quality status and trends in Europe. Atmos. Environ. 98, 376–384. https://doi.org/10.1016/j.atmosenv.2014.09.017.

Hildebrandt Ruiz, L., Yarwood, G., 2013. Interactions between Organic Aerosol and NOy: Influence on Oxidant Production., Prepared for the Texas AQRP (Project 12-012). University of Texas at Austin, and ENVIRON International Corporation, Novato, CA.

IMO, 2008a. Nitrogen oxides (NOx) - Regulation 13. http://www.imo.org/en/OurWork/Environment/PollutionPrevention/AirPollution/Pages/Nitrogen-oxides-(NOx)-%E2%80%93-Regulation-13.aspx.

IMO, 2008b. Sulphur oxides (SOx) and particulate matter (PM) - regulation 14. http://www.imo.org/en/OurWork/Environment/PollutionPrevention/AirPollution/Pages/Sulphur-oxides-(SOx)-%E2%80%93-Regulation-14.aspx.

Jimenez, P., Baldasano, J.M., 2004. Ozone response to precursor controls in very complex terrains: use of photochemical indicators to assess O_3-NO_x-VOC sensitivity in the northeastern Iberian Peninsula. J. Geophys. Res.-Atmos., 109 https://doi.org/10.1029/2004jd004985.

Jonson, J.E., Simpson, D., Fagerli, H., Solberg, S., 2006. Can we explain the trends in European ozone levels? Atmos. Chem. Phys. 6, 51–66. https://doi.org/10.5194/acp-6-51-2006.

Jonson, J.E., Gauss, M., Jalkanen, J.P., Johansson, L., 2019. Effects of strengthening the Baltic Sea ECA regulations. Atmos. Chem. Phys. 19, 13469–13487. https://doi.org/10.5194/acp-19-13469-2019.

Karl, M., Jonson, J.E., Uppstu, A., Aulinger, A., Prank, M., Sofiev, M., Jalkanen, J.P., Johansson, L., Quante, M., Matthias, V., 2019. Effects of ship emissions on air quality in the Baltic Sea region simulated with three different chemistry transport models. Atmos. Chem. Phys. 19, 7019–7053. https://doi.org/10.5194/acp-19-7019-2019.

Kuenen, J.J.P., Visschedijk, A.J.H., Jozwicka, M., Denier van der Gon, H.A.C., 2014. TNO-MACC_II emission inventory; a multi-year (2003–2009) consistent high-resolution European emission inventory for air quality modelling. Atmos. Chem. Phys. 14, 10963–10976. https://doi.org/10.5194/acp-14-10963-2014.

Li, Y., Lau, A.K.H., Fung, J.C.H., Zheng, J.Y., Liu, S.C., 2013. Importance of NOx control for peak ozone reduction in the Pearl River Delta region. J. Geophys. Res.-Atmos. 118, 9428–9443. https://doi.org/10.1002/jgrd.50659.

Lv, Z.F., Liu, H., Ying, Q., Fu, M.L., Meng, Z.H., Wang, Y., Wei, W., Gong, H.M., He, K.B., 2018. Impacts of shipping emissions on $PM_{2.5}$ pollution in China. Atmos. Chem. Phys. 18, 15811–15824. https://doi.org/10.5194/acp-18-15811-2018.

Mamoudou, I., Zhang, F., Chen, Q., Wang, P.P., Chen, Y.J., 2018. Characteristics of PM2.5 from ship emissions and their impacts on the ambient air: a case study in Yangshan Harbor, Shanghai. Sci. Total Environ. 640, 207–216. https://doi.org/10.1016/j.scitotenv.2018.05.261.

Matthias, V., Aulinger, A., Backes, A., Bieser, J., Geyer, B., Quante, M., Zeretzke, M., 2016. The impact of shipping emissions on air pollution in the greater North Sea region – part 2: scenarios for 2030. Atmos. Chem. Phys. 16, 759–776. https://doi.org/10.5194/acp-16-759-2016.

Mertens, M., Grewe, V., Rieger, V.S., Jockel, P., 2018. Revisiting the contribution of land transport and shipping emissions to tropospheric ozone. Atmos. Chem. Phys. 18, 5567–5588. https://doi.org/10.5194/acp-18-5567-2018.

Monks, P.S., Archibald, A.T., Colette, A., Cooper, O., Coyle, M., Derwent, R., Fowler, D., Granier, C., Law, K.S., Mills, G.E., Stevenson, D.S., Tarasova, O., Thouret, V., von Schneidemesser, E., Sommariva, R., Wild, O., Williams, M.L., 2015. Tropospheric ozone and its precursors from the urban to the global scale from air quality to short-lived climate forcer. Atmos. Chem. Phys. 15, 8889–8973. https://doi.org/10.5194/acp-15-8889-2015.

Monteiro, A., Russo, M., Gama, C., Borrego, C., 2018. How important are maritime emissions for the air quality: at European and national scale. Environ. Pollut. 242, 565–575. https://doi.org/10.1016/j.envpol.2018.07.011.

Nakatsubo, R., Oshita, Y., Aikawa, M., Takimoto, M., Kubo, T., Matsumura, C., Takaishi, Y., Hiraki, T., 2020. Influence of marine vessel emissions on the atmospheric $PM_{2.5}$ in Japan's around the congested sea areas. Sci. Total Environ. 702. https://doi.org/10.1016/j.scitotenv.2019.134744.

Nenes, A., Pandis, S.N., Pilinis, C., 1998. ISORROPIA: a new thermodynamic equilibrium model for multiphase multicomponent inorganic aerosols. Aquat. Geochem. 4, 123–152. https://doi.org/10.1023/a:1009604003981.

Oikonomakis, E., Aksoyoglu, S., Ciarelli, G., Baltensperger, U., Prévôt, A.S.H., 2018a. Low modeled ozone production suggests underestimation of precursor emissions (especially NOx) in Europe. Atmos. Chem. Phys. 18, 2175–2198. https://doi.org/10.5194/acp-18-2175-2018.

Oikonomakis, E., Aksoyoglu, S., Wild, M., Ciarelli, G., Baltensperger, U., Prevot, A.S.H., 2018b. Solar "brightening" impact on summer surface ozone between 1990 and 2010 in Europe - a model sensitivity study of the influence of the aerosol-radiation interactions. Atmos. Chem. Phys. 18, 9741–9765. https://doi.org/10.5194/acp-18-9741-2018.

Passant, N.R., 2002. Speciation of UK Emissions of Non-methane Volatile Organic Compounds. AEA Technology, Culham, Abingdon, Oxon, UK.

Pollack, I.B., Ryerson, T.B., Trainer, M., Neuman, J.A., Roberts, J.M., Parrish, D.D., 2013. Trends in ozone, its precursors, and related secondary oxidation products in Los Angeles, California: a synthesis of measurements from 1960 to 2010. J. Geophys. Res.-Atmos. 118, 5893–5911. https://doi.org/10.1002/jgrd.50472.

Ramboll, 2018. User's Guide: The Comprehensive Air Quality Model With Extensions (CAMx) Version 6.5, California.

Robinson, A.L., Donahue, N.M., Shrivastava, M.K., Weitkamp, E.A., Sage, A.M., Grieshop, A.P., Lane, T.E., Pierce, J.R., Pandis, S.N., 2007. Rethinking organic aerosols: semivolatile emissions and photochemical aging. Science 315, 1259–1262. https://doi.org/10.1126/science.1133061.

Sillman, S., 1999. The relation between ozone, NOx and hydrocarbons in urban and polluted rural environments. Atmos. Environ. 33, 1821–1845. https://doi.org/10.1016/s1352-2310(98)00345-8.

Stegehuis, A.I., Vautard, R., Ciais, P., Teuling, A.J., Miralles, D.G., Wild, M., 2015. An observation-constrained multi-physics WRF ensemble for simulating European mega heat waves. Geosci. Model Dev. 8, 2285–2298. https://doi.org/10.5194/gmd-8-2285-2015.

UNECE, 1999. The 1999 Gothenburg Protocol to Abate Acidification, Eutrophication and Ground-level Ozone. http://www.unece.org/env/lrtap/multi_h1.html.

Viana, M., Hammingh, P., Colette, A., Querol, X., Degraeuwe, B., de Vlieger, I., van Aardenne, J., 2014. Impact of maritime transport emissions on coastal air quality in Europe. Atmos. Environ. 90, 96–105. https://doi.org/10.1016/j.atmosenv.2014.03.046.

Wei, W., Li, Y., Ren, Y., Cheng, S., Han, L., 2019. Sensitivity of summer ozone to precursor emission change over Beijing during 2010–2015: a WRF-Chem modeling study. Atmos. Environ. 218, 116984. https://doi.org/10.1016/j.atmosenv.2019.116984.

WHO, 2016. Global health observatory (GHO) data: concentrations of fine particulate matter ($PM_{2.5}$). https://www.who.int/gho/phe/air_pollution_pm25_concentrations/en/.

WHO, 2019. Ten Threats to Global Health in 2019. World Health Organization https://www.who.int/news-room/feature-stories/ten-threats-to-global-health-in-2019.

Yan, Y., Pozzer, A., Ojha, N., Lin, J., Lelieveld, J., 2018. Analysis of European ozone trends in the period 1995–2014. Atmos. Chem. Phys. 18, 5589–5605. https://doi.org/10.5194/acp-18-5589-2018.